Oncogene (2014), 1–11

www.nature.com/onc

ORIGINAL ARTICLE

Structural proteins of Kaposi's sarcoma-associated herpesvirus antagonize p53-mediated apoptosis

P Chudasama[1], A Konrad[1], R Jochmann[1], B Lausen[2], P Holz[1], E Naschberger[1], F Neipel[3], N Britzen-Laurent[1] and M Stürzl[1]

The tumor suppressor p53 is a central regulatory molecule of apoptosis and is commonly mutated in tumors. Kaposi's sarcoma-associated herpesvirus (KSHV)-related malignancies express wild-type p53. Accordingly, KSHV encodes proteins that counteract the cell death-inducing effects of p53. Here, the effects of all KSHV genes on the p53 signaling pathway were systematically analyzed using the reversely transfected cell microarray technology. With this approach we detected eight KSHV-encoded genes with potent p53 inhibiting activity in addition to the previously described inhibitory effects of KSHV genes *ORF50*, *K10* and *K10.5*. Interestingly, the three most potent newly identified inhibitors were KSHV structural proteins, namely ORF22 (glycoprotein H), ORF25 (major capsid protein) and ORF64 (tegument protein). Validation of these results with a classical transfection approach showed that these proteins inhibited p53 signaling in a dose-dependent manner and that this effect could be reversed by small interfering RNA-mediated knockdown of the respective viral gene. All three genes inhibited p53-mediated apoptosis in response to Nutlin-3 treatment in non-infected and KSHV-infected cells. Addressing putative mechanisms, we could show that these proteins could also inhibit the transactivation of the promoters of apoptotic mediators of p53 such as BAX and PIG3. Altogether, we demonstrate for the first time that structural proteins of KSHV can counteract p53-induced apoptosis. These proteins are expressed in the late lytic phase of the viral life cycle and are incorporated into the KSHV virion. Accordingly, these genes may inhibit cell death in the productive and in the early entrance phase of KSHV infection.

Oncogene advance online publication, 27 January 2014; doi:10.1038/onc.2013.595

Keywords: KSHV; p53; apoptosis; reversely transfected cell microarray; early infection; lytic replication

INTRODUCTION

Kaposi's sarcoma-associated herpesvirus (KSHV) is the etiological agent of Kaposi's sarcoma[1] and of two lymphoproliferative disorders, namely primary effusion lymphoma (PEL) and multicentric castleman's disease.[2,3] KSHV virions are composed of a capsid containing the viral DNA, a surrounding tegument layer and the viral envelope containing several glycoproteins. After infection of cells, KSHV resides in a latent phase, during which only a subset of viral genes are expressed.[4,5] Viral replication and virion production take place during the lytic phase, which can be induced by various extrinsic and intrinsic stimuli. The lytic phase is divided into an immediate early, early and late lytic phase.[6,7] The majority of infected cells in Kaposi's sarcoma and PEL are harboring the virus in the latent phase. Only 3–5% of the cells exhibit the productive lytic infection phase.[8–10]

The tumor suppressor p53 is a major regulator of apoptosis and cell cycle progression. Activation of p53 is tightly controlled by its negative regulator MDM2, which is an E3 ligase directing p53 to proteasomal degradation.[11] Mutation or inactivation of p53 is typically found in many different forms of cancers, including colon, breast, lung, hematopoietic tissues and brain cancers.[12–14] In contrast, all KSHV-associated malignancies have been shown to express wild-type p53 with rare exceptions.[15,16] Accordingly, it was hypothesized that KSHV may encode proteins with p53 inhibitory functions. The latency-associated nuclear antigen-1/ORF73, viral interferon regulatory factors (vIRFs) K9/vIRF1, K10/vIRF-4 and K10.5/vIRF-3, as well as the KSHV replication and transcription activator (RTA)/ORF50, were subsequently identified as proteins that counteract p53 activity.[17–20] All of these proteins are either expressed in the latent or the immediate early lytic phase of the viral life cycle.[7] However, despite the presence of KSHV-encoded p53 inhibitory latent proteins, p53 signaling was shown to be intact in PEL cells in response to p53-activating agents, suggesting that latently expressed KSHV genes do not represent potent inhibitors of this protein.[15,21]

The presence of wild-type p53 protein in KSHV tumors and lymphomas suggested that the activation of p53 may be a promising strategy for the therapy of KSHV-associated diseases. This approach was further supported by the finding that p53 activation selectively killed latent KSHV-infected cells in comparison with uninfected and Epstein–Barr virus-infected cells.[22] Accordingly, Nutlin-3, a small molecule inhibitor of the p53-MDM2 interaction that leads to the stabilization of p53, has been employed to treat Kaposi's sarcoma and PEL in cell culture and animal models.[22–25] This approach resulted in regression of the disease but was counteracted specifically during the lytic phase of KSHV replication.[26] So far, it is not known which KSHV genes may confer resistance to p53-mediated apoptosis. Accordingly, we aimed to identify additional inhibitors of the p53 signaling pathway encoded by KSHV. To this goal, we systematically analyzed the effects of a validated cDNA expression library of all KSHV-encoded genes,[27] using reversely transfected cell microarray

[1]Division of Molecular and Experimental Surgery, Department of Surgery, University Medical Center Erlangen, Friedrich-Alexander-University Erlangen-Nürnberg, Erlangen, Germany; [2]Department of Mathematical Sciences, University of Essex, Colchester, UK and [3]Institute of Clinical and Molecular Virology, University Medical Center Erlangen, Friedrich-Alexander-University Erlangen-Nürnberg, Erlangen, Germany. Correspondence: Professor Dr M Stürzl, Division of Molecular and Experimental Surgery, Department of Surgery, University Medical Center Erlangen, Friedrich-Alexander-University Erlangen-Nürnberg, Schwabachanlage 10, D-91054 Erlangen, Germany.
E-mail: michael.stuerzl@uk-erlangen.de
Received 21 May 2013; revised 15 November 2013; accepted 13 December 2013

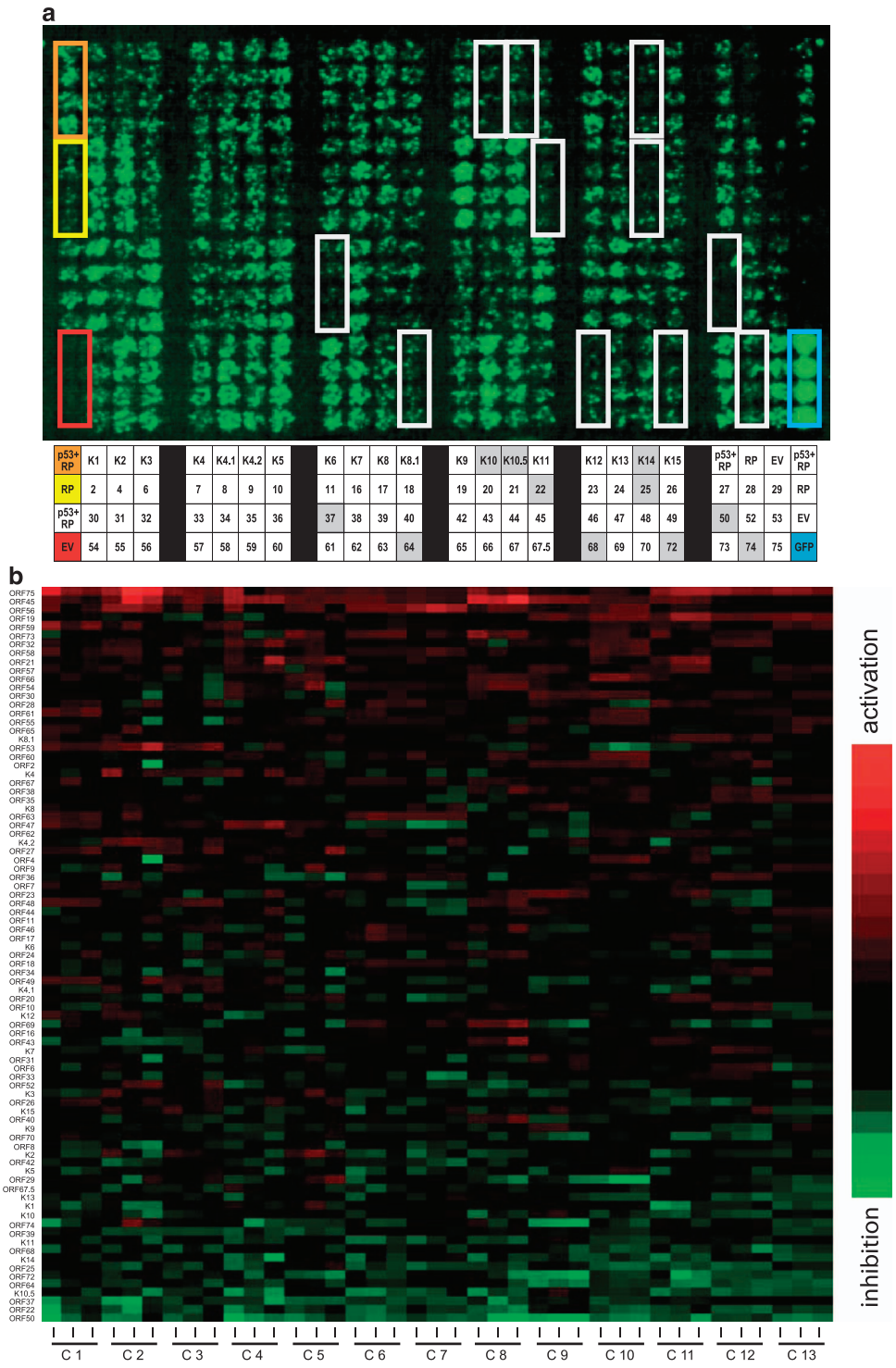

Figure 1. Identification of KSHV-encoded p53 inhibitors using RTCM. (**a**) Upper panel: representative p53 reporter assay performed with all KSHV-encoded genes in HEK 293 cells using the RTCM technique. Each transfection was performed in quadruplicates (384 transfections/cell chip). Test samples consisted of a reporter plasmid encoding GFP under the control of a p53 response element (p53-GFP), a plasmid constitutively expressing p53 in combination with expression plasmids of the different KSHV genes. Statistically significant inhibitors of p53 activity are indicated (white frames, $n = 11$). Control transfections with the empty vector control only (EV, red frame), with EV and the reporter plasmid (RP, yellow frame) or with EV, RP and the p53 expression plasmid (p53 + RP, orange frame) are indicated. A plasmid constitutively expressing GFP was used as a positive control for transfection (GFP, blue frame). (**a**) Lower panel: Respective plasmid application. Statistically significant inhibitors of p53 activity (gray) and control transfections (color code as above) are indicated. (**b**) Heat map summarizing the results of 14 976 transfection experiments. KSHV proteins were sorted according to their effects on p53 activity (red: activation, green: inhibition). Relative fluorescence intensities from three cell chips from each of the 13 independent RTCM spotting experiments (C1–C13) were analyzed using AIDA Image Analysis software. The heat map was created by employing the mean values of light arbitrary units (LAU) from all experiments using the R package for statistical computing (R core team 2012). The median of the measured four signals were transformed using the (natural) logarithm. Afterwards, the transformed signals of each of the 39 chips were standardized by subtracting the median of each chip and dividing by the interquartile difference of each chip. The genes are indicated at the left side and are ordered according to the mean values of the 39 chips.

Table 1. P53 inhibition by KSHV genes

KSHV proteins	*Fold change (p53 inhibition)*	*P-value*	*Expression profile during viral life cycle*	*Features/functions of the KSHV proteins*
ORF50	0.771	0.000004	Lytic (immediate early)	RTA
ORF22	0.832	0.0001	Lytic (late)	gH
ORF37	0.845	0.0003	Lytic (early)	SOX
K10.5	0.851	0.001	Latent (B cells)	vIRF-3
ORF64	0.851	0.0003	Lytic (late)	Large tegument protein, de-ubiquitinase
ORF72	0.853	0.0004	Latent	v-Cyc
ORF25	0.869	0.004	Lytic (late)	Major capsid protein
K14	0.88	0.0005	Lytic (delayed early)	vOX-2
ORF68	0.9	0.01	Lytic (late)	Major envelope glycoprotein
ORF74	0.91	0.02	Lytic (late)	vGPCR
K10	0.913	0.01	Lytic (early)	vIRF-4

Abbreviations: gH, glycoprotein H; KSHV, Kaposi's sarcoma-associated herpesvirus; RTA, replication and transcription activator; SOX, shutoff and exonuclease; v-Cyc, viral cyclin; vGPCR, viral G-protein coupled receptor; vIRF-3, viral interferon regulatory factor-3; vIRF-4, viral interferon regulatory factor-4; vOX-2, viral OX-2.

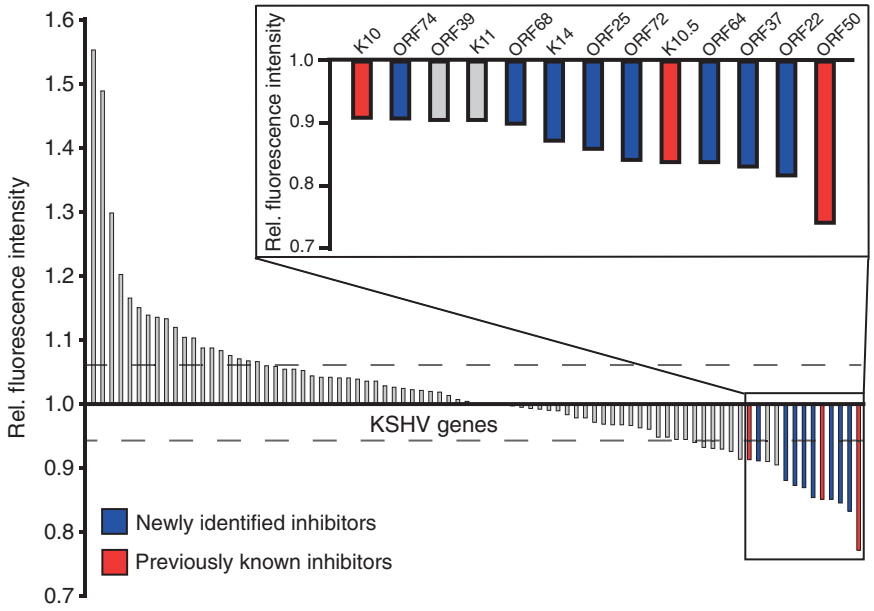

Figure 2. Graphical representation of RTCM evaluation. P53 activity is depicted as fold changes of the mean values of relative GFP fluorescence intensities derived from all experimental points (39 cell chips further comprising transfections in quadruplicates) compared with the mean value of the p53 activation control. Each bar represents mean fold change values for the respective KSHV gene. A fold change of ± 0.05 units was regarded as background activation/inhibition (broken line). KSHV proteins identified as potent inhibitors are indicated in the inset. Red bars indicate previously described p53 inhibitory KSHV proteins. Blue bars represent KSHV proteins newly identified to inhibit p53 in this study. Gray bars represent KSHV proteins that had no statistically significant inhibitory effects on p53 activity.

(RTCM) analysis as an unbiased high-throughput transfection approach.[28,29] We report the unprecedented potential of three KSHV structural proteins to inhibit p53-mediated transcriptional activation and apoptosis.

RESULTS

RTCM analysis identifies novel p53 inhibitors encoded by KSHV

In order to apply an unbiased screen for the p53 inhibitory activity of all KSHV-encoded genes, the RTCM method was used. RTCM is a high-throughput transfection technique that allows the performance of several hundred transfections in parallel using eukaryotic cells on a single glass slide.[30] Previously, we successfully used this method in order to identify novel nuclear factor-κB-activating genes encoded by KSHV.[28] Here we used the RTCM approach in order to systematically investigate which KSHV genes may inhibit p53 activity. Plasmids encoding all individual KSHV genes[27] were cotransfected in parallel into human embryonic kidney (HEK) 293 cells together with a p53 expression plasmid and an indicator plasmid expressing green fluorescent protein (GFP) under the control of a p53-response element. The effects on p53-induced GFP expression were quantified by fluorescence laser scanning. A representative cell chip of the p53 reporter assay is shown along with the spotting scheme (Figure 1a). Each combination was spotted in quadruplicates one below the other (indicated by rectangular frames). A clear induction of promoter activity was observed in the presence of p53 (Figure 1a, orange frame) as compared with transfections with the indicator plasmid alone (Figure 1a, yellow frame). Transfection of a plasmid constitutively expressing destablized GFP (pd2EGFP-N1) was used as a transfection control, demonstrating high transfection efficiency (~90%; Figure 1a, blue frame). Several KSHV genes that inhibited p53 activity under the conditions of cotransfection were detected, namely *K10*, *K10.5*, *K14*, *ORF22*, *ORF25*, *ORF37*, *ORF50*, *ORF64*, *ORF68*, *ORF72* and *ORF74*

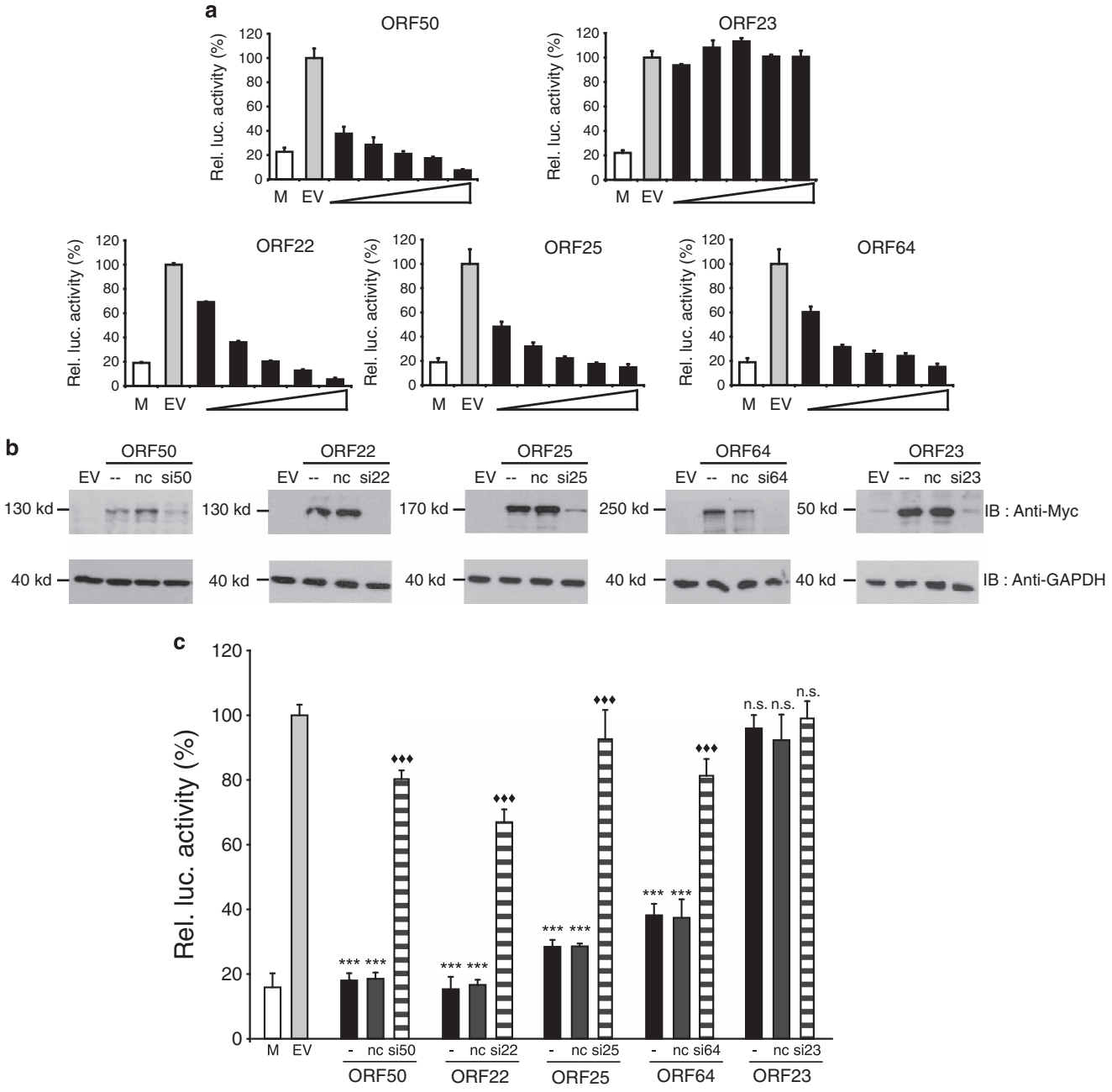

Figure 3. p53 inhibitors identified by RTCM can be confirmed by classical transfection assays. (**a**) In order to validate the results obtained in the RTCM assay, HEK 293 cells were transfected classically with increasing concentrations (0.1, 0.3, 0.7, 0.9 and 1.3 μg) of plasmids encoding the indicated KSHV proteins (black bars) together with a reporter plasmid encoding luciferase under the control of the p53 response element (p53-luc) and a plasmid constitutively expressing p53. Transfections with the indicator plasmid and either the empty vector (M, mock; white bar), or the p53 expression plasmid together with the empty vector (EV; gray bar, activation control) were used as controls. The total amount of plasmid in each transfection mix was adjusted to 3.0 μg by the addition of EV. The relative luciferase units (RLUs) were measured 48 h after transfection. Results are expressed as percent inhibition of p53 activity compared with the p53 activation control. A representative result of three independent experiments is shown. ORF50 was used as a positive control and ORF23 was used as a negative control. (**b**) HEK 293 cells were transfected with the plasmids encoding the different KSHV genes along with the respective siRNAs (siRNA against *ORF50* = si50; accordingly, the other siRNAs targeting KSHV proteins are abbreviated as si22, si25, si64 and si23). A non-targeting control siRNA was used as a negative control (nc). All siRNAs were used at 5 nM concentrations. KSHV proteins in cell lysates (20 μg) were detected via the Myc-tag by immunoblotting (IB). Detection of glyceraldehyde 3-phosphate dehydrogenase (GAPDH) was used as the loading control. Cells transfected with EV or only with the KSHV expression plasmids in the absence of siRNA (--) were used as additional controls. (**c**) HEK 293 cells were transfected with targeting (striped bars) and non-targeting (dark gray bars) siRNAs as described in **b** and, in addition, with p53-luc, a p53-expressing plasmid and plasmids encoding the indicated KSHV proteins. Transfections with p53-luc and empty vector in the absence (M, white bar) and presence (EV, light gray bar, activation control) of the p53-expressing plasmid were used as controls. Relative luciferase units (RLUs) were measured 48 h after transfection. Results are expressed as percent inhibition of p53 activity compared with the p53 activation control (EV). A representative result out of three independent experiments is shown. ORF50 was used as a positive control and ORF23 was used as a negative control. Statistical significances of inhibition (comparision to p53 activation control, ***$P \leqslant 0.0001$) and reversal (comparision to transfection with negative control siRNA, ♦♦♦$P \leqslant 0.0001$) are indicated.

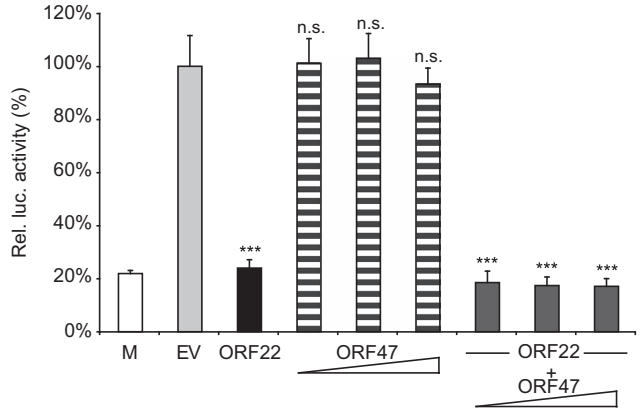

Figure 4. ORF47 does not abrogate inhibition of p53 by ORF22. In order to determine whether a complex of gH (encoded by ORF 22) and gL (encoded by ORF47) may affect p53 inhibition the ORF22 encoding plasmid (0.2 μg) was cotransfected with increasing amounts (0.1, 0.25 and 0.5 μg) of an ORF47-encoding plasmid, a reporter plasmid encoding luciferase under the control of the p53 response element (p53-luc) and a plasmid constitutively expressing p53 into HEK 293 cells (dark gray bars). Transfection of ORF22 (black bar), ORF47 alone (striped bars), as well as transfection of empty vector (EV, light gray bar) and a transfection without the p53-expressing plasmid to determine endogeneous p53 activity (M, white bar) were used as controls. The total amount of plasmid in each transfection mix was adjusted to 3.0 μg by the addition of EV. Results are expressed as percent inhibition of p53 activity compared with the EV control (***$P \leqslant 0.0001$).

(upper panel, white frames; lower panel, light gray boxes). The expression of KSHV proteins was shown using immunostaining on cell chip (Supplementary Figure S1a). Expression of KSHV genes exhibiting only weak signals on the chip was confirmed by western blotting (Supplementary Figure S1b).

In order to substantiate the results above, 13 independent repetitions of the spotting were performed, and reverse transfection was carried out with three different slides of each of the 13 batches in order to perform statistical analysis. Each individual combination was spotted in quadruplicates on each slide. Altogether, 14 976 transfections were carried out with each experimental point in 156 replications. A heat map summarizing all the results obtained in this approach showing the relative levels of p53 activity for respective KSHV genes in the different replications is depicted (Figure 1b).

Statistical analyses (*t*-test, Bonferroni correction) identified 11 genes that significantly inhibited p53 activity (Table 1). This group included the previously described p53 inhibitors ORF50, K10 and K10.5, which confirmed the validity of the screening method employed (Table 1 and Figure 2, red bars). In addition, the genes encoding ORF22, ORF25, ORF37, ORF64, ORF68, ORF72, ORF74 and K14 were identified as novel inhibitors of p53 activity (Table 1 and Figure 2, blue bars).

Structural KSHV proteins are efficient inhibitors of p53 activity

The inhibition of p53 activity by KSHV genes observed in the RTCM analyses was confirmed in classical transfection experiments (Supplementary Figure S2). Expression plasmids encoding the newly identified p53-inhibiting KSHV genes were cotransfected into HEK 293 cells with a reporter plasmid encoding luciferase under the control of a p53 response element (p53-luc) and a p53 expression plasmid. Cotransfection with the established inhibitor *ORF50* (Supplementary Figure S2) was used as a positive control. All tested genes inhibited p53 activity significantly as compared with cells transfected with the empty vector (Supplementary Figure S2, gray bar). Quantitative analysis of the results showed that three structural proteins of KSHV, namely ORF22 (glycoprotein H), ORF25 (major capsid protein) and ORF64 (tegument protein), exerted the strongest p53 inhibitory activity (Supplementary Figure S2). So far, there have been no reports suggesting that structural proteins of KSHV may inhibit p53 activity. Accordingly, ORF22, ORF25 and ORF64 were analyzed in more detail.

Using the luciferase indicator system and classical transfection procedure, we tested whether the inhibitory effects of ORF22, ORF25 and ORF64 on activity of overexpressed p53 were dose-dependent, using increasing amounts of the respective expression plasmids (Figure 3a). ORF50 was used as a positive control. *ORF23*, which encodes a KSHV tegument protein, was used as a negative control, as the protein is localized in the cytoplasm analogously to ORF22, ORF25 and ORF64, but did not exert a significant effect on p53 activity in the RTCM analysis. All three structural proteins inhibited p53 activity in a dose-dependent manner similar to ORF50, whereas ORF23 had no effect, as indicated by the luciferase reporter assay (Figure 3a). HEK 293 cells are known to be transformed with and to express E1A and E1B proteins of adenovirus type 5 that have been shown to regulate p53 activity.[31,32] With the aim to rule out the influence of these adenoviral proteins on the effects of ORF22, ORF25 and ORF64, the above results were validated with the MCF7 breast cancer cell line and using Nutlin-3 treatment for the induction of endogenous p53 as an alternative approach. Moreover, in this experimental setup ORF22, ORF25, ORF64 and the positive control ORF50 significantly inhibited p53 activity, whereas ORF23 had no effect (Supplementary Figure S3a). Lactate dehydrogenase detection in the cell culture supernatants of transfected HEK 293 (Supplementary Figure S3b) and MCF7 cells (Supplementary Figure S3c) demonstrated that transfections with the different expression plasmids did not exert significant cytotoxicity.

In order to exclude that p53 inhibition was based on unspecific effects, we inhibited the expression of *ORF22, ORF25* and *ORF64*, as well as the control genes *ORF50* and *ORF23*, using specific small interfering RNAs (siRNAs; Figure 3b). In each case, the expression of the target gene was strongly reduced in the presence of the respective siRNA. In the p53-luciferase reporter assay, knockdown of ORF22, ORF25, ORF64 and ORF50 resulted in significant reversal of the inhibitory activity (Figure 3c, striped bars, $P \leqslant 0.001$) as compared with samples where a negative control siRNA was used (Figure 3c, dark gray bars, $P \leqslant 0.001$). These results confirmed the specificity of the inhibitory effect.

ORF22 (gH) retains the p53 inhibitory function in the presence of ORF47 (gL)

ORF22 (gH) forms a heterodimeric complex with ORF47 (gL) in a lytically reactive cell and is subsequently incorporated into the viral envelope.[33] This complex participates in the membrane fusion process during virus entry[33] via interactions with heparin sulfate proteoglycans and EphA2 protein.[34,35] Cotransfection of these genes also results in the ORF22/ORF47 (gH/gL) complex formation.[34] In order to investigate the effect of this complex on p53 activity, we performed the p53-reporter assay described above with ORF22 in combination with different concentrations of ORF47. The cotransfection of *ORF22/ORF47* resulted in efficient inhibition of p53 activity, thereby implying that ORF22 can exert its p53 inhibitory effects individually, as well as in a complex with ORF47 (Figure 4).

KSHV structural proteins inhibit Nutlin-3-induced apoptosis

Next, we analyzed whether ORF22, ORF25 and ORF64 may inhibit p53-mediated apoptosis. Apoptosis was induced by Nutlin-3 treatment (30 μM) using transiently transfected HEK 293 cells and KSHV-infected iSLK.219 cells.[36] After 18 h of treatment, the amount of apoptosis was analyzed by a caspase 3/7 cleavage Glo assay (Figure 5a). ORF22, ORF25 and ORF64 significantly

inhibited caspase 3/7 activation by Nutlin-3 treatment in both HEK 293 cells and infected iSLK.219 cells ($P \leqslant 0.05$, Figure 5a). ORF25, ORF64 and ORF50 significantly inhibited p53-mediated apoptosis to a similar extent in both cell types, whereas ORF22 emerged as the most potent inhibitor. The negative control protein ORF23 had no influence on apoptosis induced by Nutlin-3.

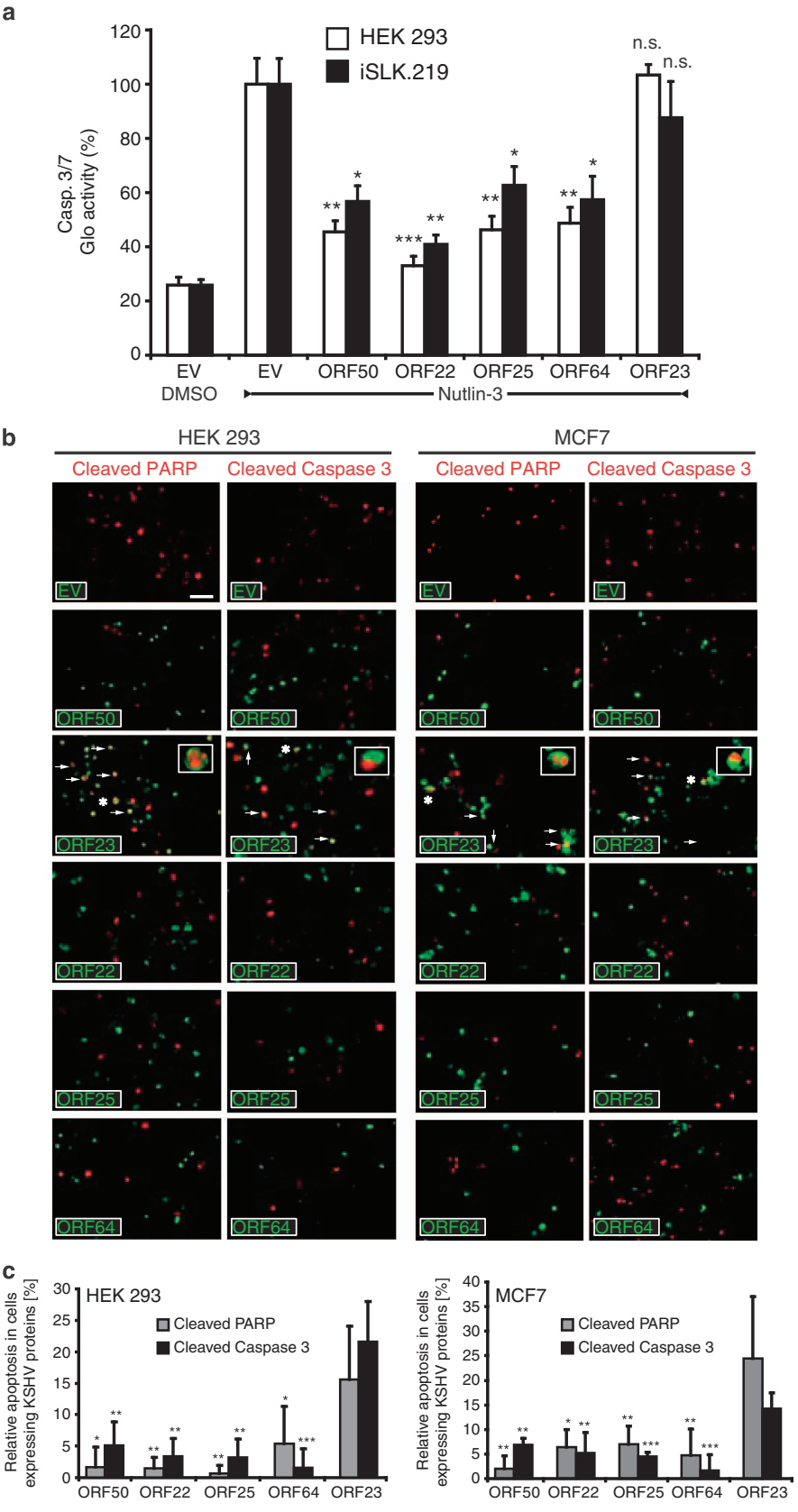

In order to verify the above results at the single-cell level, an immunofluorescence double-staining approach was applied to Nutlin-3-treated HEK 293 cells and MCF7 cells that were transfected with the different KSHV ORFs. Apoptotic cells were identified by staining of cleaved poly-(ADP-ribose) polymerase and cleaved caspase 3 (Figure 5b, red staining). The cells expressing the individual KSHV proteins were visualized by staining the Myc-tag (green staining, Figure 5b). Again, ORF50 was used as positive control and ORF23 as negative control. Cells expressing ORF22, ORF25 and ORF64 were rarely costained for cleaved poly-(ADP-ribose) polymerase and cleaved caspase 3, indicating inhibition of p53-induced apoptosis in these cells (Figure 5b). Identical results were observed with ORF50-expressing cells. In contrast, cells expressing ORF23 were frequently double stained also for cleaved poly-(ADP-ribose) polymerase or cleaved caspase 3 (Figure 5b, white arrows, inset). Quantitative evaluation confirmed that the numbers of double-stained cells were significantly lower in transfections with ORF22, ORF25, ORF64 and ORF50 as compared with ORF23 (Figure 5c). These results showed that KSHV structural proteins ORF22, ORF25 and ORF64 are potent inhibitors of p53-mediated apoptosis.

ORF22, ORF25 and ORF64 inhibit p53-mediated transactivation of BAX and PIG3

P53 is known to induce apoptosis in part by acting as a transcriptional activator of pro-apoptotic proteins BAX and PIG3.[37,38] Moreover, p53 controls the expression of its negative regulator MDM2.[39] In order to investigate molecular mechanisms involved in the anti-apoptotic activity of KSHV structural proteins, we tested their effects on the expression of BAX, PIG3 and MDM2 promoter activation by p53 using luciferase reporter assay combined with overexpression of p53 (Figure 6). ORF22, ORF25 and ORF64 significantly inhibited p53-mediated activation of BAX- and PIG3-luc promoters (Figure 6, upper and middle panel). Only moderate effects were observed on the MDM2-luc reporter (Figure 6, lower panel). In line with a previous report,[18] ORF50 strongly inhibited all three promoters tested (Figure 6, ORF50). The negative control protein ORF23 had no effect on the p53-mediated activation of the above promoters (Figure 6, ORF23). Taken together, these data suggest that inhibition of the transcription of apoptotic factors such as BAX and PIG3 contributes to the anti-apoptotic effects of ORF22, ORF25 and ORF64.

DISCUSSION

The present study describes a systematic screening approach using the RTCM method with all 85 KSHV genes to identify unknown p53 inhibitors. The RTCM method has previously been successfully applied for the systematic analyses of single and combination effects of genes encoded by KSHV to identify nuclear factor-κB activators.[28,40] Here we identified *ORF22*, *ORF25*, *ORF37*, *ORF64*, *ORF68*, ORF72, *ORF74* and *K14* as new KSHV genes that significantly ($P \leqslant 0.05$) inhibited p53 activity (Table 1). Of note, previously known p53 inhibitors ORF50, K10 and K10.5 were confirmed in this study, which validated our approach.[18–20]

Only two of previously described inhibitors, namely K9 (vIRF1)[41] and ORF73 (latency-associated nuclear antigen-1),[17] were not detected in the RTCM screening. In a subsequent classical transfection approach, K9, but not ORF73, was found to inhibit p53 activity (Supplementary Figure S4). Western blotting confirmed that ORF73 expression levels were at least as high as that observed in KSHV-infected cells (data not shown). The results regarding ORF73 are in agreement with recent findings showing that ORF73 has no impact on p53-driven transcriptional activation and apoptosis, because the ORF73:p53 interacting complex is subject to rapid disassembly upon p53 activation.[15,21,42] The discrepancy of K9 activity between RTCM and classical transfection may be attributed to differential expression levels of K9 in the two assays.

The KSHV structural proteins ORF22, ORF25 and ORF64 were identified as new potent inhibitors of p53 activity. The specificity of the three KSHV genes on p53 inhibition was shown using an siRNA approach. The three proteins significantly inhibited the effects of ectopically overexpressed p53 both in an RTCM test as well as in classical transient transfection experiments in HEK 293 cells. Putative effects of the adenovirus E1A and E1B proteins that are expressed in HEK 293 cells[31,32] could be excluded by successful reproduction of the experiments in MCF7 and iSLK.219 cell lines, which do not express the two adenoviral proteins. In these experiments, Nutlin-3 was used as an alternative exogenous activator of p53 as compared with p53 overexpression. Most importantly, all three genes protected cells from Nutlin-3-induced apoptosis as shown by caspase 3/7 cleavage-based reporter assay and at the single-cell level by immunocytochemical analysis of apoptotic markers. Under all conditions and in all three cell lines, ORF22, ORF25 and ORF64 inhibited p53-mediated apoptosis.

ORF22 encodes the glycoprotein H that is present in the viral envelope.[33] Similar to the homologs of other herpesviruses, KSHV ORF22/gH in cooperation with ORF47/gL mediates fusion during viral entry.[43–45] In contrast to most other herpesviruses, the maturation of gH to the functional protein does not depend on gL.[34] The p53 inhibitory function of ORF22 detected here was also not affected by and/or dependent on ORF47/gL (Figure 4). Anti-apoptotic functions of other herpesviral envelope glycoproteins gJ, gG (bovine herpesvirus-1) have been described.[46,47] However, structural homologs of these proteins are not present in KSHV. In the light of our data, it is conceivable that ORF22 may serve as a functional homolog of these proteins.

Figure 5. ORF22, ORF25 and ORF64 inhibit Nutlin-3-induced apoptosis. (**a**) Caspase 3/7 cleavage assay: HEK 293 (white bars) and iSLK.219 cells (black bars) were transfected with the empty vector (EV) or the indicated plasmids encoding KSHV proteins. Twenty-four hours post transfection, apoptosis was induced by treatment with Nutlin-3 (30 μM, 18 h) and detected using caspase 3/7 Glo assay. Treatment with dimethyl sulfoxide (DMSO) was used as a negative control. Relative values of caspase 3/7 Glo activity in ORF-transfected as compared with EV-transfected cells in the presence of Nutlin-3 are shown as a measure of apoptosis. Apoptosis was high in EV- and ORF23- (negative control) transfected samples and was significantly lower (**$P \leqslant 0.001$, *$P \leqslant 0.05$) in cells transfected with ORF22, ORF25, ORF64 and ORF50 (positive control). A representative result out of three independent experiments is shown. (**b**) Cleaved poly-(ADP-ribose) polymerase (PARP) and caspase 3: HEK 293 (left panel) and MCF7 (right panel) cells were transfected and treated with Nutlin-3 (30 μM for HEK 293, 5 μM for MCF7). Subsequently, cells were fixed, permeabilized and immunostained for simultaneous detection of KSHV proteins (green, Myc-epitope tag) and cleaved PARP or cleaved caspase 3 (red). Cells double-stained for KSHV proteins and simultaneously for cleaved PARP or cleaved caspase 3 were rarely detected in transfections with ORF50, ORF22, ORF25 and ORF64, but were frequently observed in the transfections with ORF23 (negative control) and are indicated (white arrows). Representative double-stained cells are marked with an asterisk and magnified in the insets. Scale bar indicates 100 μm. (**c**) Quantitative evaluation: immunofluorescence stainings of HEK 293 (left panel) and MCF7 (right panel) cells were evaluated. The total number of cells expressing KSHV proteins (stained for Myc-tag, green) and of those which in addition were positive for cleaved PARP or cleaved caspase 3 (red) were counted. For this purpose, at least four independent high-power microscopic fields were evaluated with a minimum of at least 100 ORF-expressing cells. The relative numbers of double-stained cells as compared with the numbers of cells expressing the respective ORFs were calculated and are given in percent as an indicator of apoptosis. Apoptosis was significantly repressed in ORF22-, ORF25-, ORF64- and ORF50 (positive control)-expressing cells as compared with cells expressing ORF23 (negative control). (*$P \leqslant 0.05$, **$P \leqslant 0.01$, ***$P \leqslant 0.001$).

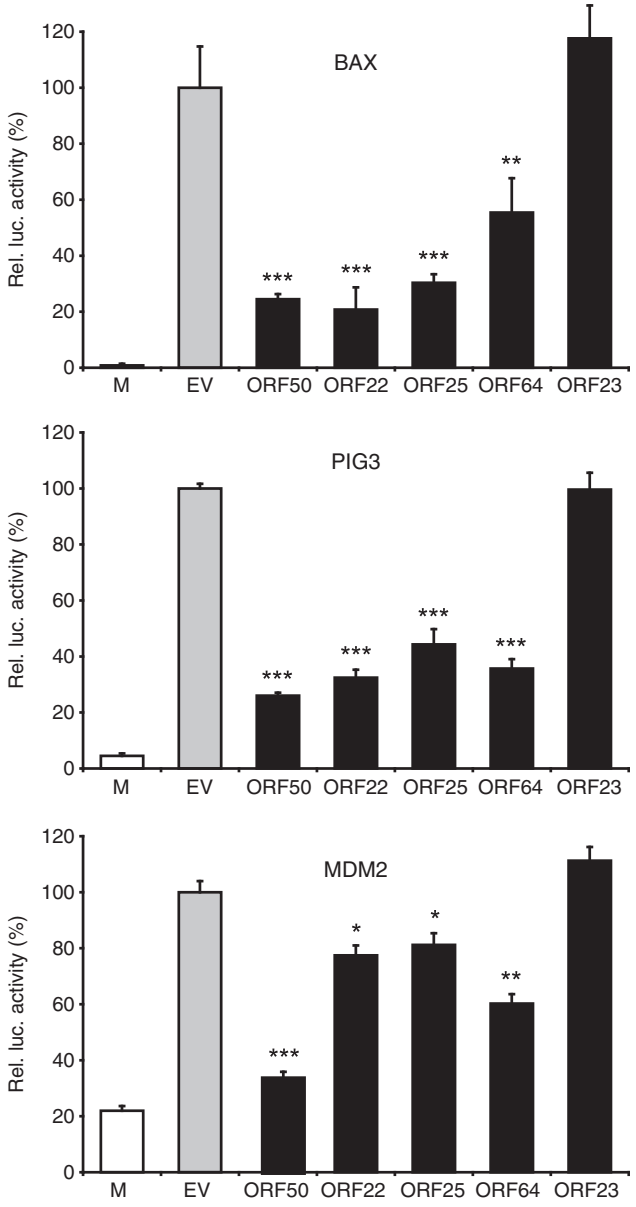

Figure 6. Structural KSHV proteins inhibit the transactivation of BAX and PIG3 promoters by p53. HEK 293 cells were transfected with reporter plasmids encoding luciferase under the control of either BAX, PIG3 or MDM2 promoters (BAX-luc, PIG3-luc and MDM2-luc) together with a p53 expression plasmid and plasmids encoding the indicated KSHV proteins (black bars) or the empty vector (EV). In order to determine endogenous p53 activity, the p53 expression plasmid was omitted (M). The results are shown relatively to the effects observed in the activation control in the presence of p53 only (EV, gray bar). A representative result out of three independent experiments is shown (***$P \leqslant 0.0001$, **$P \leqslant 0.001$, *$P \leqslant 0.01$).

ORF25 constitutes the major capsid protein of KSHV and is the most abundant protein in the capsid.[48] ORF25 is well conserved throughout herpesviruses. Expression of this gene is a marker of lytic replication and has been detected in the few lytically infected cells in Kaposi's sarcoma.[8] Recently, ORF25 has been shown to be modified by *O*-linked N-acetylglucosamine;[49] the functional role of this is yet to be elucidated. Interestingly, capsid proteins of RNA viruses such as West Nile virus and Rubella virus have been shown to inhibit apoptosis.[50,51] In addition, the capsid protein (HBcAg) of hepatitis B virus can counteract p53 activity.[52] Here we describe for the first time an anti-apoptotic activity of a herpesviral capsid protein.

ORF64 serves as a scaffolding hub protein during the tegumentation and secondary envelope formation process, eventually occupying the inner tegument that is tethered to the capsid.[53,54] ORF64 expression in the viral life cycle starts in the early lytic phase.[4] Its extensive role in the tegumentation process implies continuous expression until the late lytic phase. Apart from this, ORF64 also functions as a de-ubiquitinase and was recently shown to inhibit RIG-I-mediated interferon-signaling by decreasing RIG-I ubiquitination.[55] Interestingly, activation of interferon-signaling has been shown to increase p53 expression and activation in response to viral infection.[56] Hence, the inhibition of interferon-signaling by ORF64 may contribute to its p53 antagonizing effect.

In order to address the functional mechanisms of how the three KSHV structural proteins may affect apoptosis, we investigated their effects on BAX and PIG3, which are both transcriptionally regulated by p53.[37,38] BAX is the mediator of mitochondrial apoptosis[57] and PIG3 is a critical component of DNA damage response pathway.[38] We demonstrated that ORF22, ORF25 and ORF64 inhibited the p53-induced transcription of both genes. Interestingly, recent reports established BAX and PIG3 as targets of Nutlin-3.[58,59] Accordingly, the inhibitory effects of the structural proteins on BAX and PIG3 may explain the resistance to Nutlin-3 treatment observed in our experiments and in KSHV-infected lytically reactive PEL cells.[26]

The lytic replication phase is critical for the pathogenic activity of KSHV. It ensures the propagation and spread of the virus.[10,60] In fact, KSHV DNA replication has been shown to be abrogated by the onset of premature apoptosis.[61] Hence, it is plausible that KSHV anti-apoptotic proteins ORF22, ORF25 and ORF64 may protect the cells from apoptotic stimuli prevailing in the lytic phase, thereby allowing the efficient production of virus particles.[62,63]

In addition, apoptosis is an important defense mechanism of the host cell in the response to the *de novo* viral infection.[64–66] The presence of the anti-apoptotic structural proteins ORF22, ORF25 and ORF64 in the virion may counteract the host cell apoptotic machinery in the very early phase of infection, before the *de novo* synthesis of viral proteins. In agreement with this, it has been postulated that the tegument protein encoded by ORF75 may induce nuclear factor-κB activation required for establishing of latency in the early steps of infection.[28,67] In fact, KSHV structural proteins gK8.1A and gB proteins have been shown to be able to modulate host cell signaling via activation of several downstream effectors during early phases of infection.[68]

In conclusion, our systematic approach revealed that KSHV structural proteins can inhibit p53 activity and apoptosis. The fact that KSHV encodes for several p53 inhibitors may reflect the important role and the manifold activation pathways of p53. Targeting ORF22, ORF25 and ORF64 in the course of molecular therapy strategies may act as a double-edged sword by reducing virus replication and survival of infected cells. Combination treatment strategies with Nutlin-3 may lead to the elimination of both latent and lytic subsets of infected cells.[69–71]

MATERIALS AND METHODS

Cell lines

HEK 293 and HEK 293T cells were purchased from ATCC (Manassas, VA, USA). iSLK.219 cells[36] were kindly provided by Don Ganem (Infectious Diseases Research, Novartis Institute for Biomedical Research, Emeryville, CA, USA). The SLK cell line used to generate iSLK.219 cells was recently identified as the renal carcinoma cell line Caki-1 using short tandem repeat profiling.[72] MCF7 cells were kindly provided by PD Dr Reiner Strick and PD Dr Pamela Strissel (University Medical Center Erlangen, Department of Obstetrics and Gynecology, Erlangen, Germany). Authenticity of all cell lines was analyzed by short tandem repeat profiling.[72] All cell lines were cultivated in Dulbecoo's modified Eagle's medium (PAA Laboratories, Pasching, Austria) supplemented with 10% fetal calf serum (Biochrom,

Berlin, Germany), 2 mM L-glutamine at 37 °C and 8.5% CO_2. For reverse transfection of HEK 293 cells, 100 U/ml penicillin and 100 μg/ml streptomycin (both from PAA Laboratories) were added to the medium. For iSLK.219, 1 μg/ml puromycin (Carl Roth, Karlsruhe, Germany), 250 μg/ml G418 (PAA Laboratories) and 250 μg/ml hygromycin (Roche, Mannheim, Germany) was additionally added. All cells were tested negative for mycoplasma.

Plasmids and siRNAs

Construction of KSHV expression library was previously described.[27,28] P53-luc construct (pp53-TA-Luc, PT3511-5W, sold as part of catalog number 631914) was purchased from Clontech (Mountain View, CA, USA). MDM2-luc plasmid was kindly provided by Professor Moshe Oren (Weizmann Institute of Science, Rehovot, Israel), BAX-luc by Professor Wafik S El-Deiry (Penn State Hershey Cancer Institute, Hershey, PA, USA) and PIG3-luc by Professor Bert Vogelstein (John Hopkins University, Baltimore, MD, USA). The p53-GFP reporter construct was cloned in the pcDNA4 plasmid (Invitrogen, Karlsruhe, Germany) by replacing the cytomegalovirus promoter and Myc-His coding sequences with p53 response element and TA minimal promoter excised from the p53-luc plasmid and GFP143 (U55761) coding sequences. The pd2EGFP-N1 plasmid (PT3206-5, catalog number 6009-1) was purchased from Clontech. All siRNA contructs were purchased from Ambion-Life Technologies (Carlsbad, CA, USA).

Sequences of siRNAs targeting KSHV genes were as follows:
ORF50: 5′-CAACCACCGCAAUGCGUUA-3′;
ORF22: 5′-GGCUUUAACUUUUCUCAGA-3′;
ORF25: 5′-GAACAAUGGUUGGAAAUAU-3′;
ORF64: 5′-CCAACACUCUAAAAGUUAU-3′; and
ORF23: 5′-GCGUCUAUGUUCUACAUGA-3′.

Silencer Select Negative Control No. 1 siRNA (catalog number 4390844; Ambion-Life Technologies) was used for non-targeting siRNA control.

Reverse transfection

Reverse transfection was performed as described previously.[27,28,73,74] Briefly, transfection complexes were prepared using Lipofectamine 2000 (Invitrogen, Darmstadt, Germany), combined with stabilizing agents and printed on slides using VersArray Chipwriter robot (Bio-Rad, Munich, Germany). These slides were then overlaid with HEK 293 cells. Forty-eight hours after transfection, slides with cell monolayer (cell chips) were collected, fixed and scanned at 25 μm resolution with Fuji FLA-5000 laser scanner (Fujiflim, Düsseldorf, Germany) to measure GFP fluorescence intensity. Fluorescence intensities were evaluated using the AIDA software (Version 4.15; Raytest, Straubenhardt, Germany) using uniform circular regions of interest for each transfection. Mean background signal from empty vector control was subtracted from the test values.

Statistical analysis

Data preprocessing was done using the R package for statistical computing (R core team 2012). The median of the four measured signals were transformed using the (natural) logarithm. Afterwards, the transformed signals of each of the 39 cell chips were standardized by subtracting the median of each chip and dividing by the interquartile difference of each chip. Differential expression between each gene and p53 was measured by the difference of the standardized signals of two to four replicates of p53, each gene minus the mean p53 signal. One sample *t*-tests were performed for the mean differences of the 13 experiments. Genes with *P*-values $<5\%$ (significant univariate *t*-test) were used as candidates for further experimental investigations.

Luciferase assay

Luciferase assay was performed as described previously.[75] HEK 293 cells were seeded in six-well plates. Next day, cells were transfected with 3 μg of total DNA using calcium phosphate transfection. After 48 h, cells were lysed using 1 × passive lysis buffer (Promega, Mannheim, Germany). The firefly luciferase activity was detected using Luciferase assay system (Promega) and Luminoskan Ascent instrument (Thermo Scientific, Langenselbold, Germany). The results were normalized to relative luciferase units detected by transfection of empty vector with the luciferase reporter plasmid. Each assay was performed in triplicates and the *P*-value was calculated using Student's *t*-test (PASW Statistics Version 18; SPSS, Inc., Chicago, IL, USA).

Cell viability

Cell viability was analyzed by determination of lactate dehydrogenase activity in the conditioned medium 48 h post transfection of the plasmids using a commercially available assay (CytoTox 96 nonradioactive cytotoxicity assay; Promega) according to the manufacturer's protocol.

Western blotting

Western blotting was performed as described previously,[76] using 20 μg lysate per lane. KSHV proteins were detected using Myc 9B11-epitope tag antibody (catalog number 2276, 1:1000 diluted, purchased from Cell Signaling, Beverly, MA, USA). Glyceraldehyde 3-phosphate dehydrogenase antibody (Catalog number MAB374, 1:40 000 diluted, purchased from Merck Millipore, Billerica, MA, USA) was used as a loading control.

Caspase 3/7 Glo assay

HEK 293 and iSLK.219 cells were seeded into clear-bottom white-walled 96-well plates (Corning, Tewksbury, MA, USA). Cells were transfected 24 h later with 0.2 μg DNA per well using FuGENE (Promega) according to the manufacturer's instructions. Twenty-four hours after transfection, cells were treated with 30 μM Nutlin-3 or dimethyl sulfoxide for 18 h. Caspase cleavage assay was performed using Caspase 3/7 Glo assay (Promega) according to the manufacturer's instructions, and luciferase activity was detected using Luminoskan Ascent instrument (Thermo Scientific).

Immunofluorescence assay

HEK 293 or MCF7 cells were seeded in chamber slides and transfected 24 h later using calcium–phosphate method or Lipofectamine 2000, respectively. After 48 h, cells were treated with Nutlin-3 (30 μM for HEK 293 and 5 μM for MCF7 cells) for 18 h. Afterwards, cells were fixed with paraformaldehyde and permeabilized with 0.1% saponin. Nonspecific binding sites were blocked using 10% goat-normal serum (Dianova, Hamburg, Germany). All primary antibodies were purchased from Cell Signaling. KSHV proteins were detected using an anti-Myc-tag antibody described above (diluted 1:3000). Apoptotic cells were detected using anti-cleaved poly-(ADP-ribose) polymerase antibodies (catalog number 9541 or 5625, diluted 1:400) and anti-cleaved caspase 3 antibodies (catalog number 9661, diluted 1:200) as primary antibodies. For detection of primary antibodies, Alexa 488 and Alexa 546 conjugated secondary antibodies were used (Invitrogen). Fluorescence images were acquired using the TCS SPE confocal microscope and the LAS-LAF software (Leica Microsystems, Wetzlar, Germany).

CONFLICT OF INTEREST

The authors declare no conflict of interest.

ACKNOWLEDGEMENTS

We thank Professor Moshe Oren, Professor Wafik S El-Deiry and Professor Bert Vogelstein for sharing plasmids. In addition, we thank PD Dr Reiner Strick and PD Dr Pamela Strissel (University Medical Center Erlangen, Department of Obstetrics and Gynecology) for providing the MCF7 cells. This work was supported by grants of the German Federal Ministry of Education and Research (BMBF, Polyprobe-Study), the Deutsche Forschungsgemeinschaft (DFG-GRK1071, STU238/6-1, SFB796 (sub-project B9)) and the German Cancer Aid (109510). Additional support was obtained from the Interdisciplinary Center for Clinical Research (IZKF) and the Emerging Fields Initiative of the Friedrich-Alexander University of Erlangen to MS, by a grant for the promotion of young researchers (ELAN) of the University Medical Center Erlangen to AK and a grant of the 'Programm zur Förderung der Chancengleichheit für Frauen in Forschung und Lehre (FFL)' to PC.

REFERENCES

1 Chang Y, Cesarman E, Pessin MS, Lee F, Culpepper J, Knowles DM *et al.* Identification of herpesvirus-like DNA sequences in AIDS-associated Kaposi's sarcoma. *Science* 1994; **266**: 1865–1869.
2 Cesarman E, Chang Y, Moore PS, Said JW, Knowles DM. Kaposi's sarcoma-associated herpesvirus-like DNA sequences in AIDS-related body-cavity-based lymphomas. *N Engl J Med* 1995; **332**: 1186–1191.
3 Soulier J, Grollet L, Oksenhendler E, Cacoub P, Cazals-Hatem D, Babinet P *et al.* Kaposi's sarcoma-associated herpesvirus-like DNA sequences in multicentric Castleman's disease. *Blood* 1995; **86**: 1276–1280.

4 Dittmer DP. Transcription profile of Kaposi's sarcoma-associated herpesvirus in primary Kaposi's sarcoma lesions as determined by real-time PCR arrays. *Cancer Res* 2003; **63**: 2010–2015.
5 Dittmer DP. Restricted Kaposi's sarcoma (KS) herpesvirus transcription in KS lesions from patients on successful antiretroviral therapy. *MBio* 2011; **2**: e00138–11.
6 Sun R, Lin SF, Staskus K, Gradoville L, Grogan E, Haase A *et al.* Kinetics of Kaposi's sarcoma-associated herpesvirus gene expression. *J Virol* 1999; **73**: 2232–2242.
7 Schulz TF, Chang Y. KSHV gene expression and regulation. In: Arvin A, Campadelli-Fiume G, Mocarski E, Moore PS, Roizman B, Whitley R *et al.* (eds). *Human Herpesviruses: Biology, Therapy, and Immunoprophylaxis*. Chapter 28, Cambridge University Press: Cambridge, 2007.
8 Staskus KA, Zhong W, Gebhard K, Herndier B, Wang H, Renne R *et al.* Kaposi's sarcoma-associated herpesvirus gene expression in endothelial (spindle) tumor cells. *J Virol* 1997; **71**: 715–719.
9 Stürzl M, Blasig C, Schreier A, Neipel F, Hohenadl C, Cornali E *et al.* Expression of HHV-8 latency-associated T0.7 RNA in spindle cells and endothelial cells of AIDS-associated, classical and African Kaposi's sarcoma. *Int J Cancer* 1997; **72**: 68–71.
10 Blasig C, Zietz C, Haar B, Neipel F, Esser S, Brockmeyer NH *et al.* Monocytes in Kaposi's sarcoma lesions are productively infected by human herpesvirus 8. *J Virol* 1997; **71**: 7963–7968.
11 Piette J, Neel H, Marechal V. Mdm2: keeping p53 under control. *Oncogene* 1997; **15**: 1001–1010.
12 Hollstein M, Sidransky D, Vogelstein B, Harris CC. p53 mutations in human cancers. *Science* 1991; **253**: 49–53.
13 Lane DP. Cancer. p53, guardian of the genome. *Nature* 1992; **358**: 15–16.
14 Levine AJ, Momand J, Finlay CA. The p53 tumour suppressor gene. *Nature* 1991; **351**: 453–456.
15 Petre CE, Sin SH, Dittmer DP. Functional p53 signaling in Kaposi's sarcoma-associated herpesvirus lymphomas: implications for therapy. *J Virol* 2007; **81**: 1912–1922.
16 Tornesello ML, Biryahwaho B, Downing R, Hatzakis A, Alessi E, Cusini M *et al.* TP53 codon 72 polymorphism in classic, endemic and epidemic Kaposi's sarcoma in African and Caucasian patients. *Oncology* 2009; **77**: 328–334.
17 Friborg Jr J, Kong W, Hottiger MO, Nabel GJ. p53 inhibition by the LANA protein of KSHV protects against cell death. *Nature* 1999; **402**: 889–894.
18 Gwack Y, Hwang S, Byun H, Lim C, Kim JW, Choi EJ *et al.* Kaposi's sarcoma-associated herpesvirus open reading frame 50 represses p53-induced transcriptional activity and apoptosis. *J Virol* 2001; **75**: 6245–6248.
19 Lee HR, Toth Z, Shin YC, Lee JS, Chang H, Gu W *et al.* Kaposi's sarcoma-associated herpesvirus viral interferon regulatory factor 4 targets MDM2 to deregulate the p53 tumor suppressor pathway. *J Virol* 2009; **83**: 6739–6747.
20 Rivas C, Thlick AE, Parravicini C, Moore PS, Chang Y. Kaposi's sarcoma-associated herpesvirus LANA2 is a B-cell-specific latent viral protein that inhibits p53. *J Virol* 2001; **75**: 429–438.
21 Chen W, Hilton IB, Staudt MR, Burd CE, Dittmer DP. Distinct p53, p53:LANA, and LANA complexes in Kaposi's sarcoma--associated herpesvirus lymphomas. *J Virol* 2010; **84**: 3898–3908.
22 Sarek G, Kurki S, Enback J, Iotzova G, Haas J, Laakkonen P *et al.* Reactivation of the p53 pathway as a treatment modality for KSHV-induced lymphomas. *J Clin Invest* 2007; **117**: 1019–1028.
23 Ye F, Lattif AA, Xie J, Weinberg A, Gao S. Nutlin-3 induces apoptosis, disrupts viral latency and inhibits expression of angiopoietin-2 in Kaposi sarcoma tumor cells. *Cell Cycle* 2012; **11**: 1393–1399.
24 Vassilev LT. Small-molecule antagonists of p53-MDM2 binding: research tools and potential therapeutics. *Cell Cycle* 2004; **3**: 419–421.
25 Vassilev LT, Vu BT, Graves B, Carvajal D, Podlaski F, Filipovic Z *et al.* In vivo activation of the p53 pathway by small-molecule antagonists of MDM2. *Science* 2004; **303**: 844–848.
26 Sarek G, Ma L, Enback J, Jarviluoma A, Moreau P, Haas J *et al.* Kaposi's sarcoma herpesvirus lytic replication compromises apoptotic response to p53 reactivation in virus-induced lymphomas. *Oncogene* 2013; **32**: 1091–1098.
27 Sander G, Konrad A, Thurau M, Wies E, Leubert R, Kremmer E *et al.* Intracellular localization map of human herpesvirus 8 proteins. *J Virol* 2008; **82**: 1908–1922.
28 Konrad A, Wies E, Thurau M, Marquardt G, Naschberger E, Hentschel S *et al.* A systems biology approach to identify the combination effects of human herpesvirus 8 genes on NF-kappaB activation. *J Virol* 2009; **83**: 2563–2574.
29 Kuhn E, Naschberger E, Konrad A, Croner RS, Britzen-Laurent N, Jochmann R *et al.* A novel chip-based parallel transfection assay to evaluate paracrine cell interactions. *Lab Chip* 2012; **12**: 1363–1372.
30 Ziauddin J, Sabatini DM. Microarrays of cells expressing defined cDNAs. *Nature* 2001; **411**: 107–110.
31 Graham FL, Smiley J, Russell WC, Nairn R. Characteristics of a human cell line transformed by DNA from human adenovirus type 5. *J Gen Virol* 1977; **36**: 59–74.
32 Moran E. Interaction of adenoviral proteins with pRB and p53. *FASEB J* 1993; **7**: 880–885.
33 Naranatt PP, Akula SM, Chandran B. Characterization of gamma2-human herpesvirus-8 glycoproteins gH and gL. *Arch Virol* 2002; **147**: 1349–1370.
34 Hahn A, Birkmann A, Wies E, Dorer D, Mahr K, Stürzl M *et al.* Kaposi's sarcoma-associated herpesvirus gH/gL: glycoprotein export and interaction with cellular receptors. *J Virol* 2009; **83**: 396–407.
35 Hahn AS, Kaufmann JK, Wies E, Naschberger E, Panteleev-Ivlev J, Schmidt K *et al.* The ephrin receptor tyrosine kinase A2 is a cellular receptor for Kaposi's sarcoma-associated herpesvirus. *Nat Med* 2012; **18**: 961–966.
36 Myoung J, Ganem D. Generation of a doxycycline-inducible KSHV producer cell line of endothelial origin: maintenance of tight latency with efficient reactivation upon induction. *J Virol Methods* 2011; **174**: 12–21.
37 Miyashita T, Reed JC. Tumor suppressor p53 is a direct transcriptional activator of the human bax gene. *Cell* 1995; **80**: 293–299.
38 Polyak K, Xia Y, Zweier JL, Kinzler KW, Vogelstein B. A model for p53-induced apoptosis. *Nature* 1997; **389**: 300–305.
39 Barak Y, Juven T, Haffner R, Oren M. mdm2 expression is induced by wild type p53 activity. *EMBO J* 1993; **12**: 461–468.
40 Stürzl M, Konrad A, Sander G, Wies E, Neipel F, Naschberger E *et al.* High throughput screening of gene functions in mammalian cells using reversely transfected cell arrays: review and protocol. *Comb Chem High Throughput Screen* 2008; **11**: 159–172.
41 Nakamura H, Li M, Zarycki J, Jung JU. Inhibition of p53 tumor suppressor by viral interferon regulatory factor. *J Virol* 2001; **75**: 7572–7582.
42 Leidal AM, Cyr DP, Hill RJ, Lee PW, McCormick C. Subversion of autophagy by Kaposi's sarcoma-associated herpesvirus impairs oncogene-induced senescence. *Cell Host Microbe* 2012; **11**: 167–180.
43 Pertel PE. Human herpesvirus 8 glycoprotein B (gB), gH, and gL can mediate cell fusion. *J Virol* 2002; **76**: 4390–4400.
44 Hutchinson L, Browne H, Wargent V, Davis-Poynter N, Primorac S, Goldsmith K *et al.* A novel herpes simplex virus glycoprotein, gL, forms a complex with glycoprotein H (gH) and affects normal folding and surface expression of gH. *J Virol* 1992; **66**: 2240–2250.
45 Spaete RR, Perot K, Scott PI, Nelson JA, Stinski MF, Pachl C. Coexpression of truncated human cytomegalovirus gH with the UL115 gene product or the truncated human fibroblast growth factor receptor results in transport of gH to the cell surface. *Virology* 1993; **193**: 853–861.
46 Jerome KR, Chen Z, Lang R, Torres MR, Hofmeister J, Smith S *et al.* HSV and glycoprotein J inhibit caspase activation and apoptosis induced by granzyme B or Fas. *J Immunol* 2001; **167**: 3928–3935.
47 Nakamichi K, Kuroki D, Matsumoto Y, Otsuka H. Bovine herpesvirus 1 glycoprotein G is required for prevention of apoptosis and efficient viral growth in rabbit kidney cells. *Virology* 2001; **279**: 488–498.
48 Nealon K, Newcomb WW, Pray TR, Craik CS, Brown JC, Kedes DH. Lytic replication of Kaposi's sarcoma-associated herpesvirus results in the formation of multiple capsid species: isolation and molecular characterization of A, B, and C capsids from a gammaherpesvirus. *J Virol* 2001; **75**: 2866–2878.
49 Jochmann R, Pfannstiel J, Chudasama P, Kuhn E, Konrad A, Stürzl M. O-GlcNAc transferase inhibits KSHV propagation and modifies replication relevant viral proteins as detected by systematic O-GlcNAcylation analysis. *Glycobiology* 2013; **23**: 1114–1130.
50 Ilkow CS, Goping IS, Hobman TC. The Rubella virus capsid is an anti-apoptotic protein that attenuates the pore-forming ability of Bax. *PLoS Pathog* 2011; **7**: e1001291.
51 Urbanowski MD, Hobman TC. The West Nile virus capsid protein blocks apoptosis through a phosphatidylinositol 3-kinase-dependent mechanism. *J Virol* 2013; **87**: 872–881.
52 Kwon JA, Rho HM. Transcriptional repression of the human p53 gene by hepatitis B viral core protein (HBc) in human liver cells. *Biol Chem* 2003; **384**: 203–212.
53 Rozen R, Sathish N, Li Y, Yuan Y. Virion-wide protein interactions of Kaposi's sarcoma-associated herpesvirus. *J Virol* 2008; **82**: 4742–4750.
54 Sathish N, Wang X, Yuan Y. Tegument proteins of Kaposi's sarcoma-associated herpesvirus and related gamma-herpesviruses. *Front Microbiol* 2012 **3**: 98.
55 Inn KS, Lee SH, Rathbun JY, Wong LY, Toth Z, Machida K *et al.* Inhibition of RIG-I-mediated signaling by Kaposi's sarcoma-associated herpesvirus-encoded deubiquitinase ORF64. *J Virol* 2011; **85**: 10899–10904.
56 Takaoka A, Hayakawa S, Yanai H, Stoiber D, Negishi H, Kikuchi H *et al.* Integration of interferon-alpha/beta signalling to p53 responses in tumour suppression and antiviral defence. *Nature* 2003; **424**: 516–523.
57 Gross A, Jockel J, Wei MC, Korsmeyer SJ. Enforced dimerization of BAX results in its translocation, mitochondrial dysfunction and apoptosis. *EMBO J* 1998; **17**: 3878–3885.

58 Kurosu T, Wu N, Oshikawa G, Kagechika H, Miura O. Enhancement of imatinib-induced apoptosis of BCR/ABL-expressing cells by nutlin-3 through synergistic activation of the mitochondrial apoptotic pathway. *Apoptosis* 2010; **15**: 608–620.
59 Voltan R, Secchiero P, Corallini F, Zauli G. Selective induction of TP53I3/p53-inducible gene 3 (PIG3) in myeloid leukemic cells, but not in normal cells, by Nutlin-3. *Mol Carcinog* (e-pub ahead of print 28 November 2012; doi: 10.1002/mc.21985).
60 Grundhoff A, Ganem D. Inefficient establishment of KSHV latency suggests an additional role for continued lytic replication in Kaposi sarcoma pathogenesis. *J Clin Invest* 2004; **113**: 124–136.
61 Austgen K, Oakes SA, Ganem D. Multiple defects, including premature apoptosis, prevent Kaposi's sarcoma-associated herpesvirus replication in murine cells. *J Virol* 2012; **86**: 1877–1882.
62 Lagunoff M, Carroll PA. Inhibition of apoptosis by the gamma-herpesviruses. *Int Rev Immunol* 2003; **22**: 373–399.
63 Moore PS. KSHV manipulation of the cell cycle and apoptosis. In: Arvin A, Campadelli-Fiume G, Mocarski E, Moore PS, Roizman B, Whitley R *et al.* (eds). *Human Herpesviruses: Biology, Therapy, and Immunoprophylaxis*. Chapter 30. Cambridge University Press: Cambridge, 2007.
64 Hanon E, Meyer G, Vanderplasschen A, Dessy-Doize C, Thiry E, Pastoret PP. Attachment but not penetration of bovine herpesvirus 1 is necessary to induce apoptosis in target cells. *J Virol* 1998; **72**: 7638–7641.
65 Morris SJ, Price GE, Barnett JM, Hiscox SA, Smith H, Sweet C. Role of neuraminidase in influenza virus-induced apoptosis. *J Gen Virol* 1999; **80**(Pt 1): 137–146.
66 Raftery MJ, Behrens CK, Muller A, Krammer PH, Walczak H, Schonrich G. Herpes simplex virus type 1 infection of activated cytotoxic T cells: induction of fratricide as a mechanism of viral immune evasion. *J Exp Med* 1999; **190**: 1103–1114.
67 de Oliveira DE, Ballon G, Cesarman E. NF-kappaB signaling modulation by EBV and KSHV. *Trends Microbiol* 2010; **18**: 248–257.
68 Chandran B. Early events in Kaposi's sarcoma-associated herpesvirus infection of target cells. *J Virol* 2009; **84**: 2188–2199.
69 Burbelo PD, Issa AT, Ching KH, Wyvill KM, Little RF, Iadarola MJ *et al.* Distinct profiles of antibodies to Kaposi sarcoma-associated herpesvirus antigens in patients with Kaposi sarcoma, multicentric Castleman disease, and primary effusion lymphoma. *J Infect Dis* 2010; **201**: 1919–1922.
70 Katano H, Sato Y, Kurata T, Mori S, Sata T. Expression and localization of human herpesvirus 8-encoded proteins in primary effusion lymphoma, Kaposi's sarcoma, and multicentric Castleman's disease. *Virology* 2000; **269**: 335–344.
71 Marcelin AG, Motol J, Guihot A, Caumes E, Viard JP, Dussaix E *et al.* Relationship between the quantity of Kaposi sarcoma-associated herpesvirus (KSHV) in peripheral blood and effusion fluid samples and KSHV-associated disease. *J Infect Dis* 2007; **196**: 1163–1166.
72 Stürzl M, Gaus D, Dirks WG, Ganem D, Jochmann R. Kaposi's sarcoma-derived cell line SLK is not of endothelial origin, but is a contaminant from a known renal carcinoma cell line. *Int J Cancer* 2013; **132**: 1954–1958.
73 Konrad A, Jochmann R, Kuhn E, Naschberger E, Chudasama P, Stürzl M. Reverse transfected cell microarrays in infectious disease research. *Methods Mol Biol* 2011; **706**: 107–118.
74 Stürzl M, Konrad A, Alkharsah KR, Jochmann R, Thurau M, Marquardt G *et al*. The contribution of systems biology and reverse genetics to the understanding of Kaposi's sarcoma-associated herpesvirus pathogenesis in endothelial cells. *Thromb Haemost* 2009; **102**: 1117–1134.
75 Naschberger E, Werner T, Vicente AB, Guenzi E, Topolt K, Leubert R *et al.* Nuclear factor-kappaB motif and interferon-alpha-stimulated response element co-operate in the activation of guanylate-binding protein-1 expression by inflammatory cytokines in endothelial cells. *Biochem J* 2004; **379**(Pt 2): 409–420.
76 Britzen-Laurent N, Lipnik K, Ocker M, Naschberger E, Schellerer VS, Croner RS *et al.* GBP-1 acts as a tumor suppressor in colorectal cancer cells. *Carcinogenesis* 2012; **34**: 153–162.

Supplementary Information accompanies this paper on the Oncogene website (http://www.nature.com/onc)